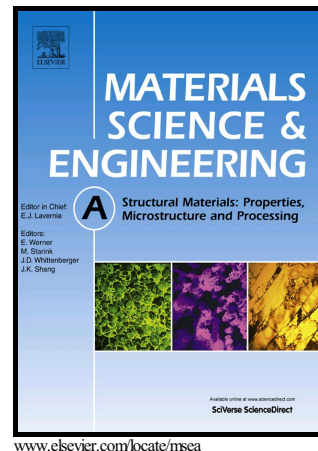


# Author's Accepted Manuscript

Formability and microstructure evolution mechanisms of Ti6Al4V alloy during a novel hot stamping process

Mateusz Kopec, Kehuan Wang, Denis J. Politis,  
Yaoqi Wang, Liliang Wang, Jianguo Lin



[www.elsevier.com/locate/msea](http://www.elsevier.com/locate/msea)

PII: S0921-5093(18)30222-3  
DOI: <https://doi.org/10.1016/j.msea.2018.02.038>  
Reference: MSA36125

To appear in: *Materials Science & Engineering A*

Received date: 28 November 2017

Revised date: 1 February 2018

Accepted date: 8 February 2018

Cite this article as: Mateusz Kopec, Kehuan Wang, Denis J. Politis, Yaoqi Wang, Liliang Wang and Jianguo Lin, Formability and microstructure evolution mechanisms of Ti6Al4V alloy during a novel hot stamping process, *Materials Science & Engineering A*, <https://doi.org/10.1016/j.msea.2018.02.038>

This is a PDF file of an unedited manuscript that has been accepted for publication. As a service to our customers we are providing this early version of the manuscript. The manuscript will undergo copyediting, typesetting, and review of the resulting galley proof before it is published in its final citable form. Please note that during the production process errors may be discovered which could affect the content, and all legal disclaimers that apply to the journal pertain.

# Formability and microstructure evolution mechanisms of Ti6Al4V alloy during a novel hot stamping process

Mateusz Kopeć<sup>1,3</sup>, Kehuan Wang<sup>\*1</sup>, Denis J. Politis<sup>1</sup>, Yaoqi Wang<sup>2</sup>, Liliang Wang<sup>\*1</sup> and Jianguo Lin<sup>1</sup>

<sup>1</sup> Department of Mechanical Engineering, Imperial College London, London SW7 2AZ, UK

<sup>2</sup> Beijing Aeronautical Manufacturing Technology Research Institute, Beijing 100024, China

<sup>3</sup> Institute of Fundamental Technological Research Polish Academy of Sciences, 02-106 Warsaw, Pawinskiego 5B, Poland

\* Corresponding author: kehuan.wang@imperial.ac.uk ; [liliang.wang@imperial.ac.uk](mailto:liliang.wang@imperial.ac.uk)

## Abstract

A novel hot stamping process for Ti6Al4V alloy using cold forming tools and a hot blank was presented in this paper. The formability of the material was studied through uniaxial tensile tests at temperatures ranging from 600 to 900 °C and strain rates ranging from 0.1 to 5 s<sup>-1</sup>. An elongation ranging from 30% to 60% could be achieved at temperatures ranging from 750 to 900°C respectively. The main microstructure evolution mechanisms varied with the deformation temperature, including recovery, phase transformation and recrystallization. The hardness of the material after deformation first decreased with the temperature due to recovery, and subsequently increased mainly due to the phase transformation. During the hot stamping tests, qualified parts could be formed successfully at heating temperatures ranging from 750 to 850°C. The forming failed at lower temperatures due to the limited ductility of the material. At temperatures higher than 900°C, extensive phase transformation of  $\alpha$  to  $\beta$  occurred during the heating. During the transfer and forming, the temperature dropped significantly which led to the formation of transformed  $\beta$ , reduction of the formability and subsequent failure. The post-form hardness distribution demonstrated the same tendency as that after uniaxial tensile tests.

**Key words:** titanium alloys, Ti6Al4V, hot stamping, microstructure

## 1. Introduction

Demand for low density and high strength materials in the aviation sector has expanded greatly due to ambitious carbon emission and fuel consumption targets. In order to meet these targets, manufacturers have focused on weight reduction via the use of lightweight materials. In the aerospace sector, low strength structural components are commonly produced from aluminium alloys, and high strength structural components are made from titanium alloys [1]. However, the forming of complex-shaped components from titanium alloys is time, energy and cost intensive. The aircraft industry currently uses methods such as superplastic forming [2], superplastic forming with diffusion bonding

[3], hot stretch forming [4], creep forming [5], hot gas-pressure forming [6] or isothermal hot forming [7, 8] to produce complex-shaped components. However, these techniques usually require a very high temperature, slow strain rate and simultaneous heating of tools and sheet during the process. These characteristics decrease productivity, and proportionally increase the cost of production. For example in conventional hot stamping using a furnace, the heating time of forming tools is approximately 2 h [9]. Research into forming technologies with increased productivity has developed processes such as the solution heat treatment, forming and in-die quenching [10], the quick-plastic forming [11], and the hot stamping using rapid heating [9,12]. One promising solution to overcome these difficulties proposed in the literature is using the hot stamping process to form complex-shaped components from sheet metal with cold dies, and rapidly quenching the workpiece in the dies simultaneously. The hot stamping process promises to reduce the tool wear commonly found in conventional hot forming processes and be an overall more efficient and economical process when compared to conventionally used isothermal hot forming techniques [9]. Traditional hot stamping processes have mainly focused on forming lightweight alloys, such as aluminium alloys and ultra-high strength steels, for the automotive industry. However few references can be found focusing on the hot stamping of titanium alloys. Recently, there has been an increased demand for titanium components in the aerospace industry due to their high strength to weight ratio, excellent temperature stability and corrosion resistance [13,14]. There is therefore a clear need to study the hot stamping of titanium alloys to achieve required mechanical performance whilst reducing manufacturing cost.

To study the hot stamping of titanium alloys, a number of studies must be performed under varying temperatures and strain rates encountered in the stamping process. The mechanical properties of these alloys are strongly dependent on the thermo-mechanical history, initial microstructure, alloy concentration and impurities within the structure [15]. Due to the high yield strength and low elastic modulus, the springback effect and shape distortion were found to be extensive upon forming thin sheets. Quan et al. [16] concluded through isothermal compression tests at temperatures ranging from 750 to 1050°C at strain rates ranging from 0.01 to 10 s<sup>-1</sup>, that the formability of titanium alloys could be increased with increasing temperature and decreased with an increase of strain rate in the lower temperature region. This phenomenon is related to the dynamic recrystallization that occurred during deformation. It was concluded that with the increase of deformation temperature, more material transforms to recrystallized structure as a result of higher mobility of grain boundaries and all grains tend to be homogeneous due to strong adaptivity for grain boundary migration. It was also shown that with the increase of strain rate, the grain size decreased. This is because the relatively low strain rates allow atoms enough time to diffuse, resulting in a lack of accumulation deformation energy and low driving force for dynamic recrystallization. At elevated temperatures, the compressive flow behaviour is characterized by a peak stress followed by strain softening. The strain softening may occur as a result of temperature increase during deformation, phase transformation and microstructural changes resulting from dynamic recovery, dynamic recrystallization and local necking [17,18]. It was found by

Bai et al. [19] that behaviour and deformation mechanisms of Ti6Al4V titanium alloy during hot forming conditions (heating temperature ranging from 820 to 1020°C, strain rates ranging from  $0.1\text{s}^{-1}$  to  $10\text{s}^{-1}$ ) are strongly dependent on initial microstructure. It was concluded that for a microstructure consisting of primary alpha phase and beta matrix, the mechanism of plastic flow softening may derive from globularization of secondary alpha phase during hot working. On the other hand, He [20] found that at temperatures ranging from 600 to 1020°C at strain rate of  $0.001\text{s}^{-1}$ , hot deformation during cooling can be used to control and refine the final recrystallized or even transformed microstructure. Though a number of publications exist related to hot stamping of titanium alloys [9, 21–23], deformation mechanisms of titanium alloys under hot stamping conditions are still not fully investigated. More knowledge and understanding of this technology and material behaviour is urgently needed to popularise and enable it to be adopted in the future.

Therefore to forward this aim, this paper presents an investigation of a hot stamping process for Ti6Al4V titanium alloy using cold forming tools and a hot blank. In order to determine the best forming conditions, uniaxial tensile tests were performed at temperatures ranging from 600 to 900°C with constant strain rates ranging from 0.1 to  $5\text{s}^{-1}$ . The hot stamping forming tests were conducted at temperatures ranging from 600 to 950°C. Microstructure evolution during tensile tests and hot stamping deformation was analysed using Scanning Electron Microscope (SEM) observations and Electron Backscatter Diffraction (EBSD) technique.

## 2. Experimental details

### 2.1 Property and microstructure characterization

Ti6Al4V titanium alloy sheet with a thickness of 1.5 mm was supplied by AVIC Beijing Aeronautical Manufacturing Technology Research Institute. Dog-bone shaped tensile specimens were fabricated according to **Fig.1**.

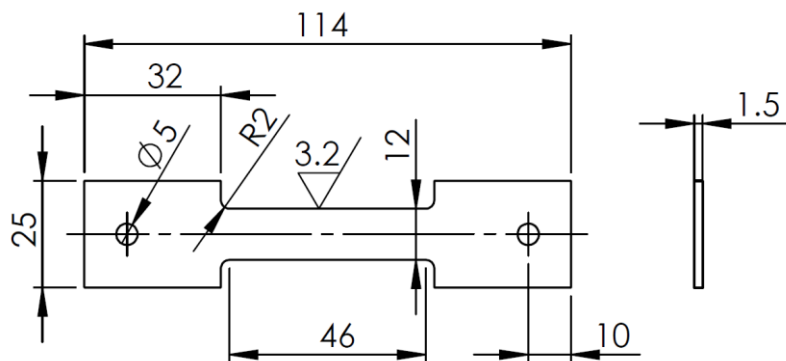


**Fig. 1** Specimen geometry for the uniaxial tensile test.

A Gleeble 3800 thermo-mechanical testing machine was used to conduct uniaxial tensile tests at elevated temperatures to characterize the properties of Ti6Al4V samples at a range of strain rates and temperatures. Samples were heated at a rate of 2°C/s to the testing temperature and deformed immediately. After failure, samples were cooled to room temperature with an average cooling rate of 40°C/s. Every test was performed at least twice to guarantee the repeatability. The Gleeble testing machine used a resistance heating method. As a result, non-uniform temperature distribution along the tensile direction was observed. Therefore, three K-type thermocouples were used to determine the uniform temperature region. Based on the obtained results, the length of the uniform temperature region was around 25 mm, which was assumed to be the effective gauge length. Hence deformation measurements and microstructure observations were focused in this area. Two lines were marked on the sample within the effective gauge area before the test, and the distance between the two lines before and after test was measured respectively to calculate the elongation. During the tests, thermocouples were welded in the center of the specimen to control and monitor the temperature. The specimen was put between two stainless steel grips, which were positioned and clamped between the Gleeble jaws. In order to obtain an accurate stress-strain curve, a C-Gauge transducer was used to measure and record the width at the center of the specimen throughout the tensile test. The true strain can be deduced by the width change and cross-sectional dimensions. The force was measured by a load cell fixed to the static jaw of the Gleeble. The true stress was determined by the instantaneous force and cross-sectional area. The required actuator stroke was set at each time increment of the test to achieve the target strain rate. This was done by assuming an effective gauge length of 25 mm in the specimen. The most critical data acquired and recorded during the tests included the C-Gauge readings of the width and the load history. The true stress and strain could then be calculated using these values and the initial dimensions of the specimen. The tensile test at room temperature was also performed with Gleeble. The C-Gauge transducer was used to get the strain. The yield strength and Young modulus were measured from the curves.

The Vickers hardness values of the specimens after the uniaxial tensile tests and hot stamping forming were measured by means of a Zwick hardness tester at room temperature with 6 measurements per condition. Each hardness measurement was performed using a 10 kgf force and the dwelling time of 10 seconds. The microstructure of investigated material was characterized by SEM and EBSD. The samples for both SEM and EBSD characterization were prepared by conventional metallographic procedures for titanium, which included hot mounting, grinding and polishing. After the mounting, the sample was ground by a Struers® polishing machine using 600, 800, 1200 and 4000 SiC papers. The initial polishing was carried out using Metrep® Durasilk M cloth, 3µm diamond polishing solution and water based lubricant. The final polishing was performed using Metrep® MD-Chem cloth and 0.04 µm Colloidal Silica solution. Volume fraction of coexisting phases was measured by ImageJ software.

## 2.2 Hot stamping of titanium alloy

To verify the feasibility of the proposed technology, forming tests were conducted on a 250 ton Instron press. The setup of facilities for hot stamping is presented in **Fig .2**. These tests were conducted at a speed of 10 mm/s at room temperature and at heating temperatures ranging from 600 to 950°C. The specimen size was 90\*8\*1.5 mm. The heating and forming temperature was monitored by welding a thermocouple wire on the specimen. Once the temperature of the specimen was stable, it was removed from the furnace, transferred to the forming tool and formed immediately by cold dies. The transfer time from the furnace to the cold die was controlled to be around 3s. The formed specimen was held for 5 s within the die. Then the formed specimen was removed from the stamping tool to allow further cooling in air to room temperature.

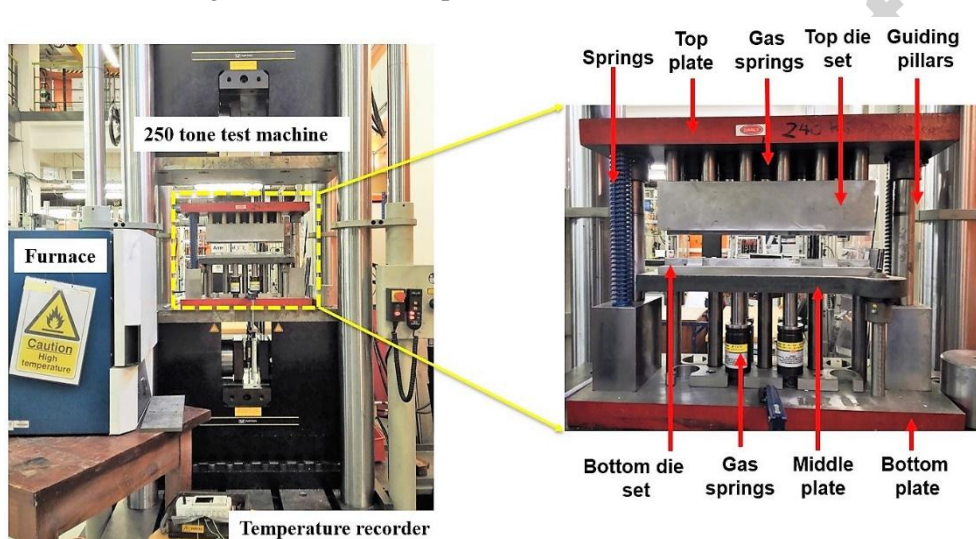


**Fig.2** Setup of facilities for hot stamping experiment.

## 3. Results

### 3.1 Initial material

The tensile test results for the as-received titanium alloy Ti6Al4V at room temperature is shown in **Fig. 3**. The results show an ultimate tensile stress for the tested material of 1120 MPa, a yield strength of 850 MPa and Young's modulus of 97 GPa. The hardness of the as-received material was measured to be 360HV10.

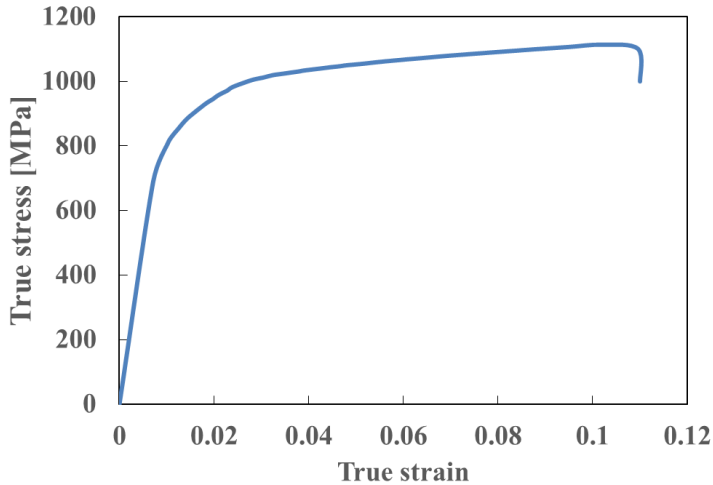


**Fig.3** Stress - strain curve obtained for as received material at the room temperature.

A microstructural investigation of the as-received material was performed on the SEM using Backscattered Electron (BSE) mode. The initial microstructure is presented in **Fig. 4**. The microstructure of the investigated titanium alloy contains the  $\alpha$ -phase matrix and small particles of  $\beta$ -phase.

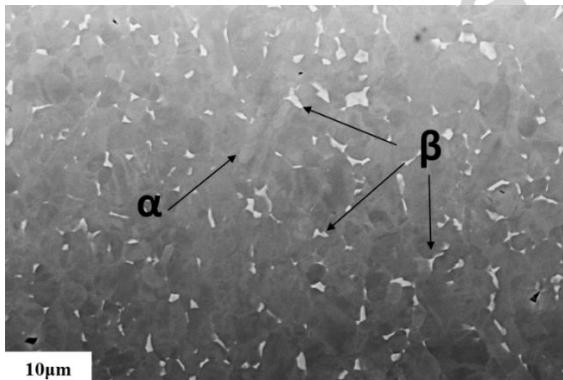


**Fig.4** SEM microstructure images of the as-received material.

### 3.2 Flow behaviour of Ti6Al4V alloy

To investigate the formability of Ti6Al4V alloy, tensile tests were performed under a range of temperatures (600 - 900°C) with a strain rate of  $1\text{s}^{-1}$  (**Fig. 5**). It was observed that the temperature has a great influence on the elongation. In the range of temperatures from 600 to 700°C, there is little change in elongation. However, for temperatures greater than 700°C, the elongation increased dramatically from 30% at 750°C to 60% at 900°C as shown in **Fig. 6**. At elevated temperatures, high dislocation mobility led to an increase in ductility (**Fig. 6**). It should be mentioned that in the range of temperatures from 600 - 700°C, strain hardening occurs. At 600°C significant strain hardening is observed, leading to an UTS of 600 MPa. At 750°C and higher temperatures, the flow stress curve became flat due to the occurrence of materials softening, indicating that the deformation mechanisms vary with the deformation temperature.

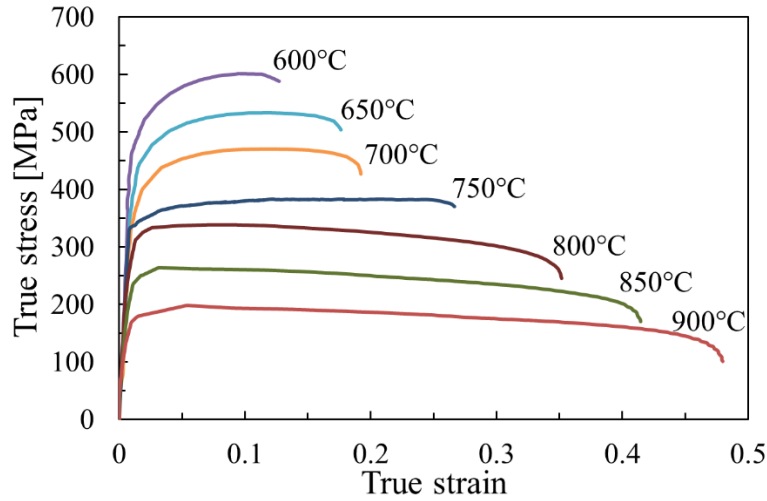


**Fig.5** Stress - strain curves obtained for Ti6Al4V samples at the range of 600 - 900°C with a constant strain rate of  $1\text{ s}^{-1}$ .

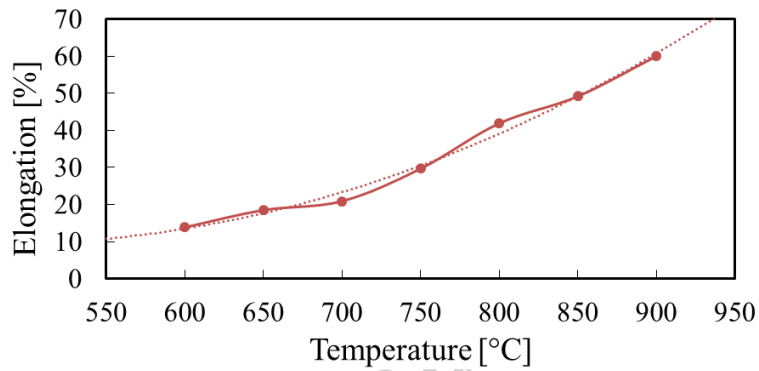


**Fig.6** Ductility obtained for Ti6Al4V samples at the range of 600 - 900°C.

It can be concluded from the above tensile test results that the material exhibits good ductility at temperatures greater than 700°C. However as the strain rate during actual forming is not constant, the material behaviour was studied through tensile tests conducted at temperatures ranging from 750 to 850°C, and strain rates ranging from  $0.1\text{ s}^{-1}$  to  $5\text{ s}^{-1}$ . **Fig. 7** presents the stress-strain curves of the initial material under different test conditions. The ductility of the investigated material increased with increasing temperature and decreasing strain rate from 0.2 at 750°C (strain rate of  $5\text{ s}^{-1}$ ) to 0.3 at strain rate of  $0.1\text{ s}^{-1}$  and from 0.4 at 850°C (strain rate of  $5\text{ s}^{-1}$ ) to 0.47 at strain rate of  $0.1\text{ s}^{-1}$ . Peak stress decreased with temperature increase and strain rate decrease from 445 MPa at 750°C to 200 MPa at 850°C. Material softening during the hot deformation process was observed, and it was found that the softening rate increased with decreasing strain rate. It could be observed that the investigated material was strongly strain rate sensitive. This phenomenon is related to the dislocation mobility and atom diffusion at higher temperatures and lower strain rate resulting in larger elongation and lower stress.

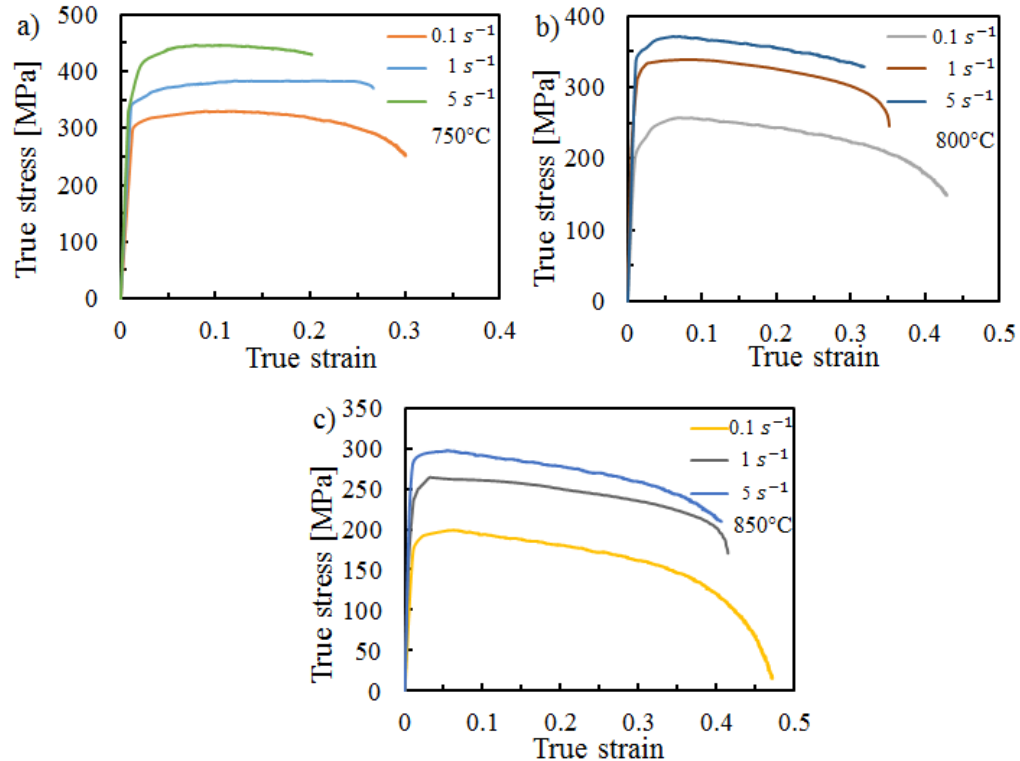


**Fig.7** Ti6Al4V stress - strain curves obtained by tensile test at different strain rate conditions for temperatures of 750°C (a), 800°C (b) and 850°C (c).

### 3.3 Properties and microstructure after deformation

Following tensile testing, the hardness distribution of all specimens was evaluated. A microstructural investigation of specimens was performed on a SEM using BSE mode. The distribution of Vickers hardness of samples following deformation at a strain rate of 1 s<sup>-1</sup> for different temperatures is shown in **Fig. 8**, and the corresponding microstructure and fraction of various phases are presented in **Fig. 9** and **Fig. 10** respectively. It can be seen that the hardness of the material decreased at first and then increased with increasing temperature. The microstructure of the investigated material showed limited change after tensile testing at temperatures of 600 and 650°C. The dimension of the  $\beta$ -phase particles and their content in the whole volume of the material were almost the same in comparison to the initial microstructure (**Fig. 9 a-b**, **Fig. 10**). This may be because the temperature was too low to initiate phase transformation. However, increased dynamic recovery occurred at higher temperature with the consumption of more dislocations, and as a result the hardness and flow stress began to decrease gradually with the increasing temperature before 750°C. When the temperature was greater than 750°C, both the content and size of  $\beta$ -phase increased with increasing temperature (**Fig. 9 d-f**, **Fig. 10**) which caused material softening during the tensile tests. Both phase transformation and recovery reduced the dislocation density resulting in a reduction in material's strength and a simultaneous increase in elongation [24]. When the sample was cooled after tensile tests, transformed beta phase and  $\alpha'$  (secondary  $\alpha$ ) formed during the cooling process which could

improve the hardness of the material at room temperature. The fraction of transformed beta increased with temperature, resulting in the simultaneous increase in hardness [25]. It is worth noting that dynamic recrystallization of  $\alpha$  grains may also occur during the deformation, which could refine the microstructure and improve the hardness [26].

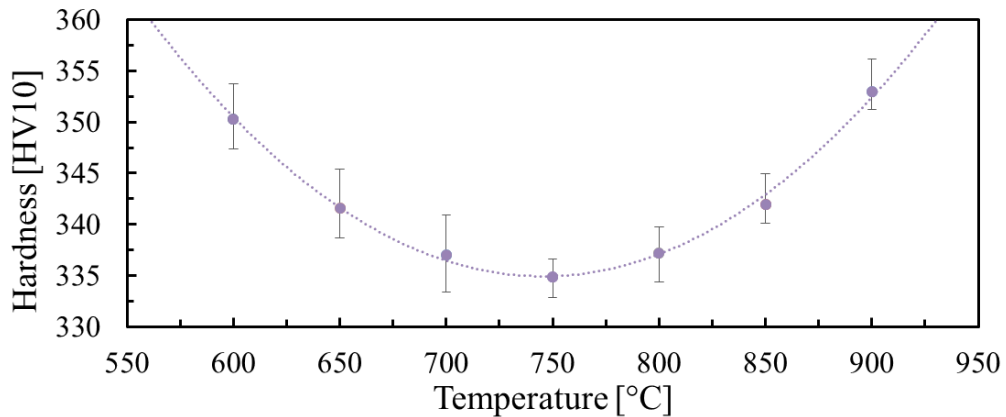


**Fig.8** Evolution of Vickers hardness of tensile tested samples conducted at different temperatures.

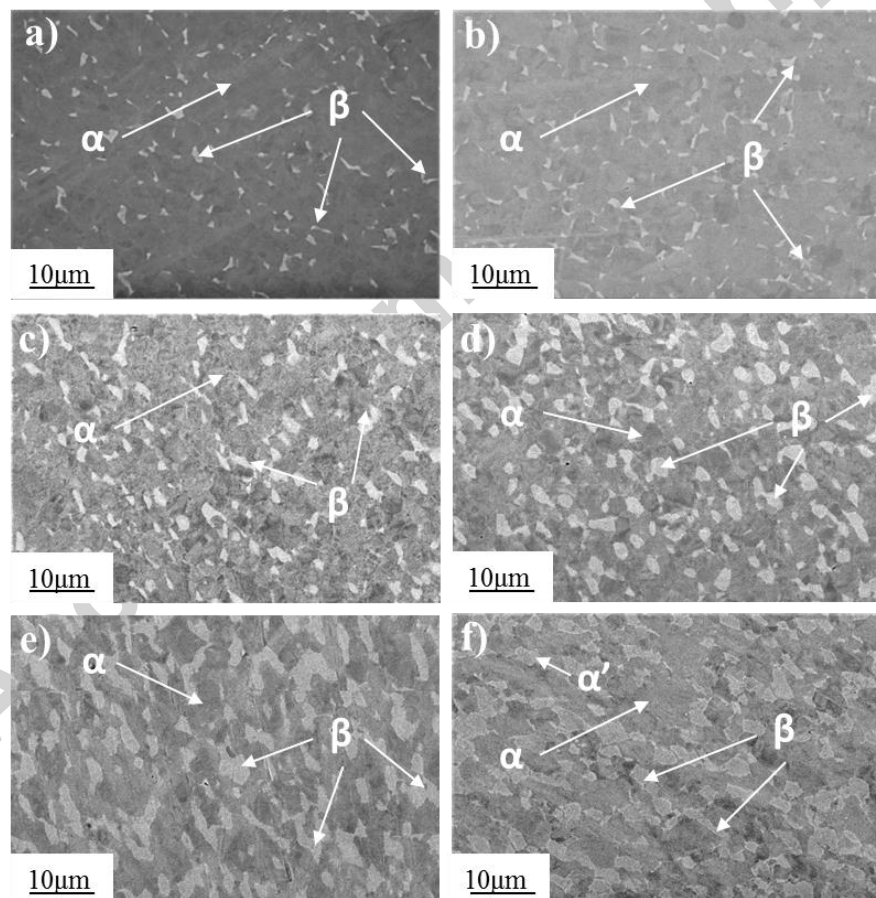


**Fig.9** SEM microstructure images of the Ti6Al4V samples tested at 600°C (a), 650°C (b), 750°C (c), 800°C (d), 850°C (e) and 900°C (f).

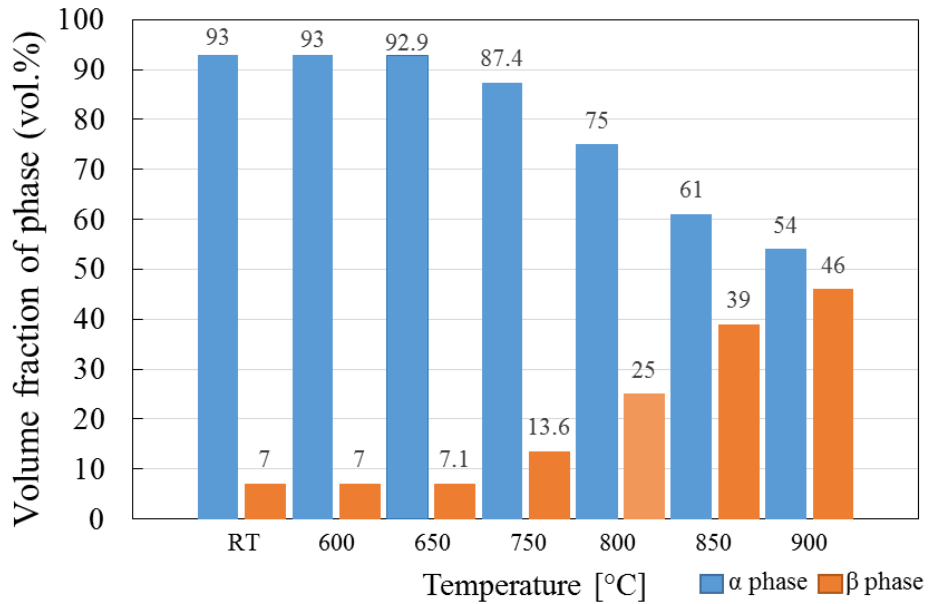


**Fig.10** Volume fraction of  $\alpha$  and  $\beta$  phase during the tensile test at different temperatures.

### 3.5 Hot stamping of titanium alloy

From the above tensile tests, it can be found that the Ti6Al4V alloy has a good formability at elevated temperature even with a high strain rate and the deformation conditions have a huge impact on the material properties. In order to further verify the feasibility of the hot stamping of titanium alloys and determine the processing windows, forming tests were conducted. The hot stamping of titanium alloy includes three main steps: heating, transfer, and simultaneously forming and quenching as shown in **Fig. 11**. During the whole forming process, temperature is one of the most important parameters, which will affect not only the formability of the material but also the post-form properties of the formed part. Therefore, a thermocouple wire was welded on the sidewall of the specimen to monitor the temperature evolution during the whole process. **Fig. 12a** presents the typical temperature history of one sample. The sample was heated to 850°C and then soaked until the temperature became stable. The total time for heating and soaking was approximately 180 s. Subsequently, it was transferred from the furnace to forming tool, formed immediately by cold dies and quenched. During the transfer, the actual temperature of the sample reduced from 850°C to approximately 700°C just before forming. During forming the temperature rapidly dropped to approximately 350°C and then gradually decreased to room temperature. **Fig. 12b** shows the load and displacement information during the forming process. The displacement curve could be divided into two parts: forming and holding. In the forming part, the press moved at a constant speed of 10 mm/s, but the load curve represented different characteristics. Before the punch contacted with the sample, the movement of the press would compress the gas spring in the dies, which led to the slow increase of load to around 10 kN. After the punch contacted with the sample, the load increased dramatically as the sample was

deformed within cold dies. After displacement reached its maximum value, the sample was held for 5 seconds within the forming tools.

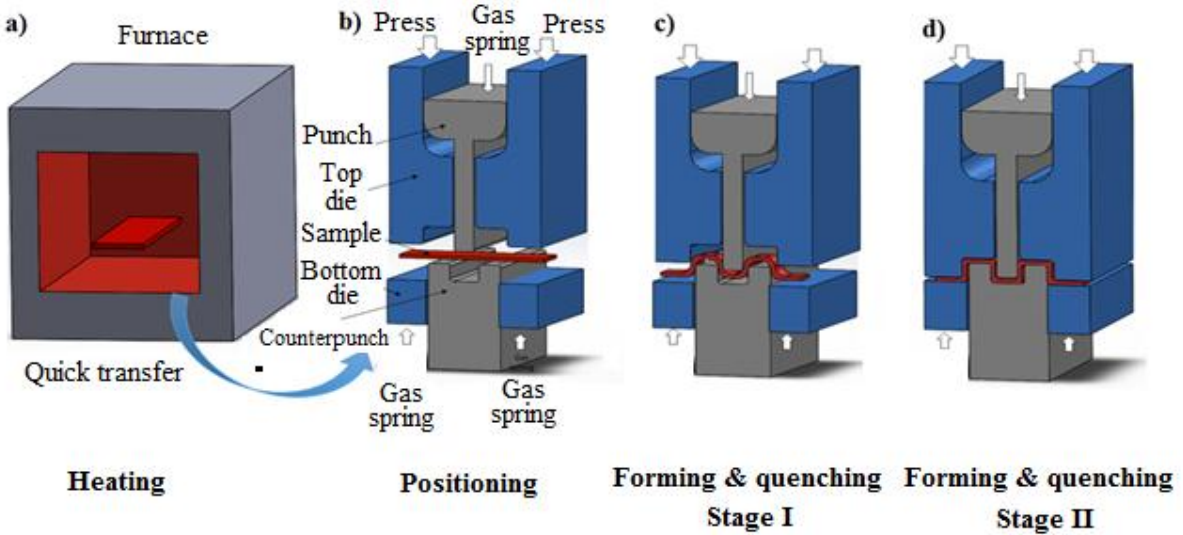


**Fig. 11** Schematic of the forming process during heating of the sample (a), at the positioning stage (b), during forming (c) and at the final stage (d).

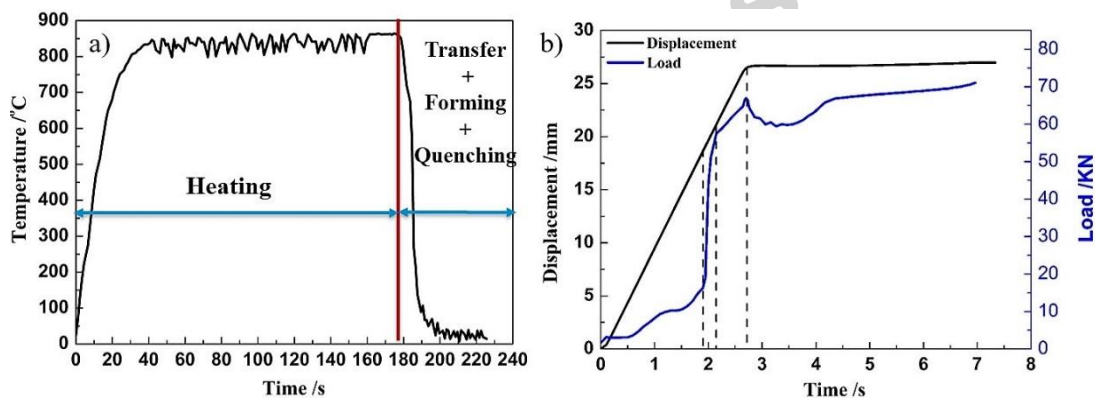


**Fig. 12** Evolution of temperature (a) and load/displacement (b) during forming process.

**Fig. 13** shows the cross-section of the formed parts using cold forming tools at different temperatures. Titanium features have been formed with heating temperatures ranging from 600 to 950°C (**Fig. 13b-f**) since room temperature forming led to the fracture of the sample into several pieces (**Fig. 13a**). A qualified part could only be formed between heating temperatures ranging from 750 to 850°C with sample heated to 600°C and formed, displaying cracks on the surface indicating that forming temperature was too low to form the component (**Fig. 14a**). Obvious cracks (**Fig. 14b**) were also observed in parts heated to 900°C and formed. When the heating temperature was increased to 950°C, the forming also failed due to the occurrence of cracking (**Fig. 13f**). This tendency is different to the uniaxial tensile tests, where the elongation increased with increasing temperature. During the tensile tests, the sample was deformed under isothermal condition, whereas the temperature

reduced significantly during the transfer and forming stages of hot stamping. The formability of the material is determined by its microstructure under certain conditions, therefore one can infer that the crack and failure that occurred at 900 and 950°C was caused by the temperature dropping and the corresponding microstructure alteration. The detailed explanation of this can be found in Section 3.6.

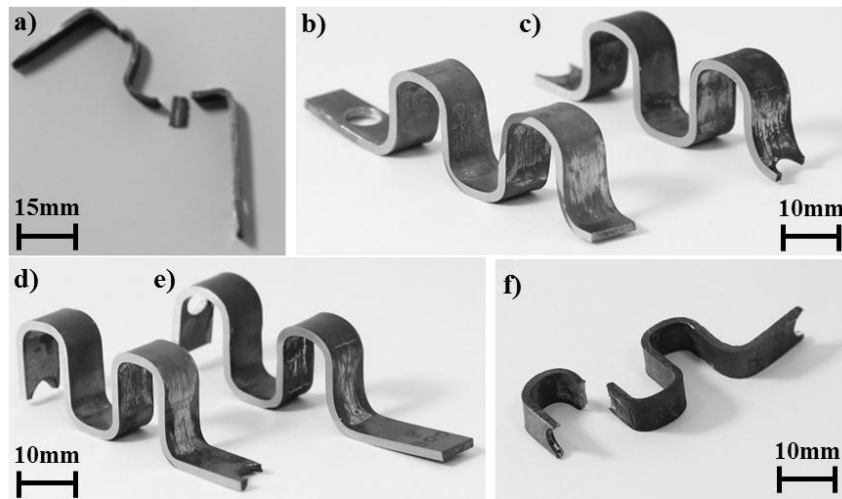


**Fig. 13** View of part formed at room temperature (a), and heating temperatures of 600°C (b), 750°C (c), 850°C (d), 900°C (e) and 950°C (f).

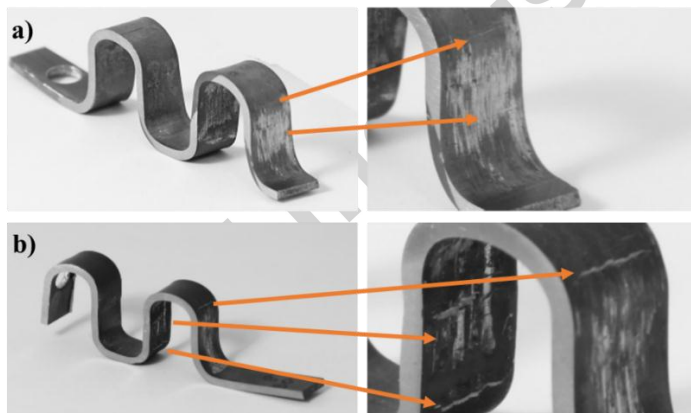


**Fig. 14** View of cracks of parts formed at heating temperature of 600°C (a) and 900°C (b).

### 3.6 Post-form properties of the formed parts under hot stamping conditions

Hardness tests were conducted on the formed parts to evaluate the post-form properties of the as-formed part, and the results are shown in **Fig. 15**. The microstructure of the formed parts and the fraction of different phases are shown in **Fig. 16** and **Fig. 17**, respectively. It can be seen that the hardness values increased from 341HV10 at 750°C to 392HV10 at 950°C (**Fig. 15**) due to phase transformation (**Fig. 16**, **Fig. 17**), which is in good agreement with the tensile test results (**Fig. 9**, **Fig. 10**). It could be observed that the microstructure of the formed part changed little after forming at temperature of 600°C. The fraction of the  $\beta$ -phase in the whole volume of the material and the dimension of its particles were almost the same as compared with the initial microstructure (**Fig. 16**,

**Fig. 17).** When the heating temperature was increased, significant phase transformation occurred and the content of  $\beta$ -phase increased dramatically from 6.7% at 600°C to 58% at 950°C as shown in **Fig. 17**.

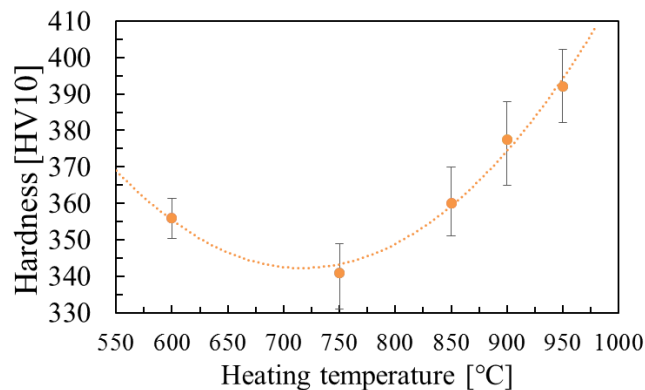


**Fig. 15** Post-form strength of components formed at different heating temperatures

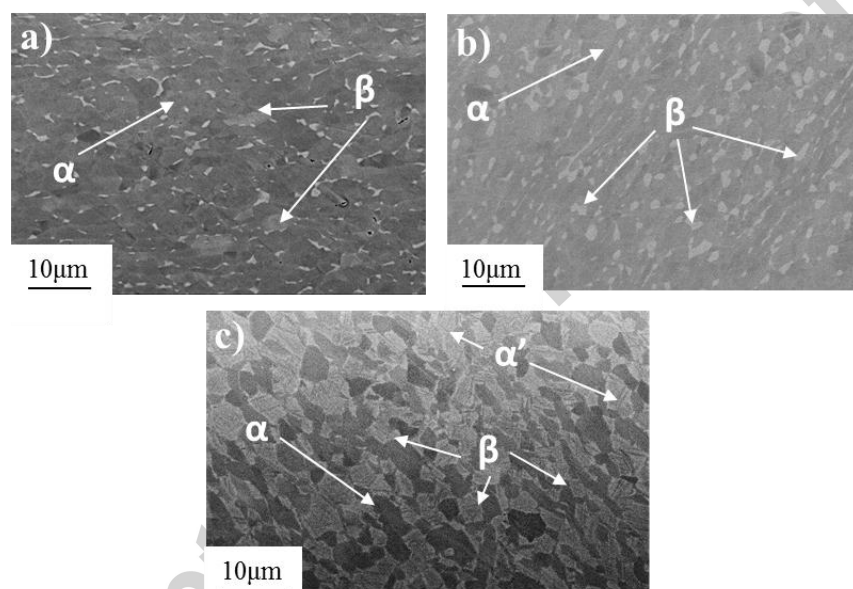


**Fig. 16** SEM microstructure images of the Ti6Al4V samples formed at heating temperatures of 600°C (a), 850°C (b), and 950°C (c).

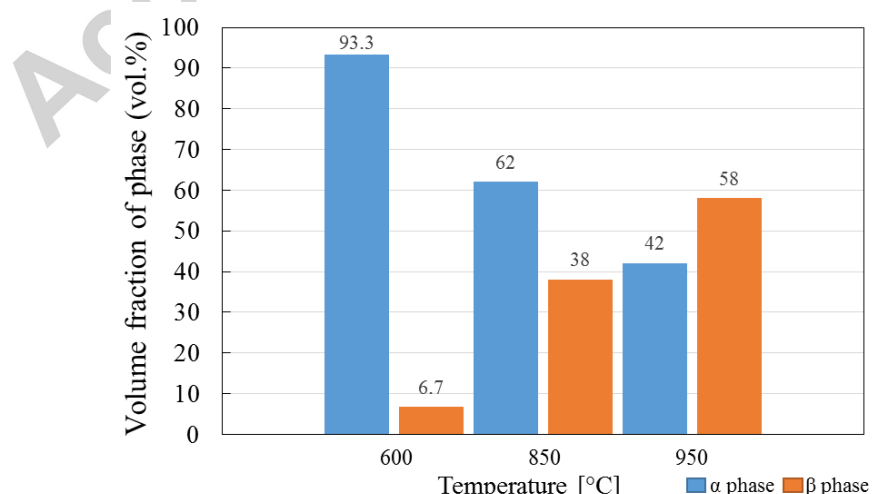


**Fig. 17** Volume fraction of  $\alpha$  and  $\beta$  phase during forming at different heating temperatures.

During thermo-mechanical processing of metals, recovery, recrystallization and phase transformation are three important microstructure evolution mechanisms. The SEM results above revealed that obvious phase transformation took place when the temperature was greater than 750°C. To further verify whether recrystallization occurred, Kernel Average Misorientation (KAM) map was captured by EBSD as shown in **Fig. 18**, where the blue colour represents low values of misorientation while the green colour represents large values. It can be observed that the average KAM values tended to decrease with increasing heating temperature and the average grain size of  $\alpha$  grains decreased first (**Fig. 18c**) and then increased (**Fig. 18d**). The initial material (**Fig. 18a**) before the forming process consisted of grains with relatively high KAM value. It indicates that the dislocation density of the initial material was high [27]. When the forming temperature increased to 850°C (**Fig. 18b**), many fine grains with low KAM value appeared, demonstrating the occurrence of recrystallization. At this stage, the temperature was high enough to initiate the recrystallization nucleation. With the temperature increasing to 900°C (**Fig. 18c**), recrystallization became more obvious, leading to grain refinement. At the temperature of 950°C (**Fig. 18d**), secondary  $\alpha$  precipitated in the  $\beta$  matrix and the equiaxed  $\alpha$  grains grew coarser. This is because significant phase transformation of  $\alpha$  to  $\beta$  took place at 950°C, which led to the secondary  $\alpha$  phase precipitates during the cooling stage. The high temperature also intensified the diffusion process and led to the merging of adjacent  $\alpha$  grains [28], which resulted in the noticeable increase of the  $\alpha$  phase grain size. Both refinement of microstructure and transformed  $\beta$  phase could improve the hardness at room temperature. Therefore when the temperature was lower than 900°C, the hardness increase may be caused by the recrystallization and phase transformation. At 950°C, the hardness increase was mainly caused by the phase transformation [16 - 17]. Both the possible grain growth during heating and the transformed  $\beta$  formed during the stamping process reduced the formability of the material, which led to the forming failure when the heating temperature was greater than 900 °C.

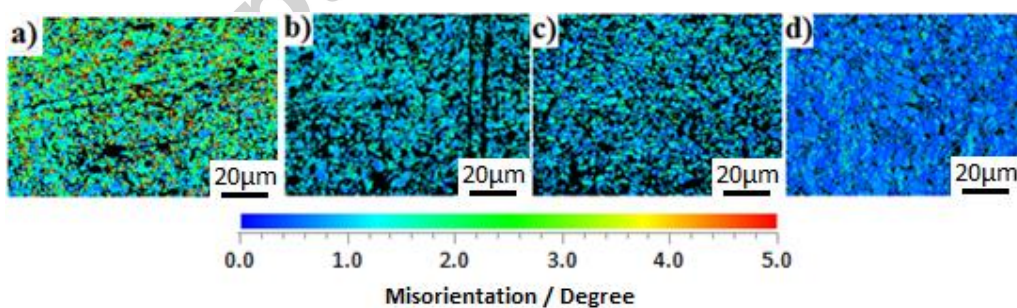


**Fig. 18** KAM maps of the material in the initial state (a) and after forming at different heating temperatures: 850°C (b), 900°C (c) and 950°C.

#### 4. Discussion

##### 4.1 Microstructure evolution mechanisms of titanium alloys under hot stamping conditions

One can find from both tensile and hot stamping test results that both the formability and post-form properties varied greatly with the deformation conditions, indicating that deformation mechanisms under different conditions may be different. Based on the obtained results, the mechanisms for Ti6Al4V alloy under hot stamping conditions were summarized in **Table 1**.

At heating temperatures ranging from 600 to 700°C, work hardening was observed (**Fig. 5**) during tensile tests, and the microstructure morphology changed little after deformation, indicating that the main mechanism was recovery. At heating temperatures ranging from 750 to 900°C, work hardening disappeared and material softening appeared during the tensile tests. After the deformation, the fraction of  $\beta$  phase and post-form hardness increased with the temperature; recrystallization of  $\alpha$  grains was also observed, and therefore the main mechanism at this temperature range would be phase transformation and recrystallization. When the heating temperature was greater than 900°C, significant phase transformation of  $\alpha$  to  $\beta$  and noticeable grain growth of  $\alpha$  grains occurred, which increased the post-form hardness and simultaneously reduced the formability of the material. Therefore, the main mechanism at this temperature range would be phase transformation and recrystallization. Similar conclusions were also reported by Ning et al. [18].

**Table 1** Microstructure evolution mechanisms for Ti6Al4V alloy under hot stamping conditions

Temperature (°C)	600 - 700	750 - 900	> 900
Microstructure morphology evolution	Little change	Phase transformation of $\alpha$ to $\beta$ and recrystallization of $\alpha$ grains	Phase transformation of $\alpha$ to $\beta$ and grain growth of $\alpha$ grains
Post-form hardness	Decrease with the temperature	Increase with the temperature	Increase with the temperature
Main mechanisms	Recovery	Phase transformation and recrystallization	Phase transformation and recrystallization

#### 4.2 Determination of processing windows for hot stamping of Ti6Al4V alloy

It can be seen from the hot stamping tests that the qualified part cannot be formed when the heating temperature was lower than 750°C or higher than 850°C, but can be formed between 750°C and 850°C as shown in **Fig. 19**, where green colour represents safe forming zone and the orange colour represents dangerous forming zone. The formability of the material was determined by both deformation conditions and the corresponding microstructure. Therefore it is very important to fully understand the relationship between the forming process and microstructure evolution. The hot stamping process is a non-isothermal forming process, and the temperature varied in different stages as shown in **Fig. 19**. The heating temperature was higher than the temperature before forming due to the temperature drop during the transfer. There would be microstructure evolution during the heating,

soaking and transfer stages before forming. Hence the heating and soaking condition would determine the microstructure before forming, and the heating temperature and temperature drop during transfer would determine the initial forming temperature. The microstructures of the material at different stages formed at heating temperatures of 850 and 950°C are shown in **Fig. 19**. It can be seen that despite the considerable drop of temperature during manual transfer from furnace to forming tools during the forming process, the microstructure changed little during the transfer. Moreover, the microstructure of the material after heating and soaking was also very similar with that after forming, even at the heating temperature of 950°C. It can be concluded that both formability and post-form properties of the material were mainly determined by the heating temperature and soaking time. Therefore both formability and post-form properties of the material could be tailored through the control of the forming process and material microstructure.

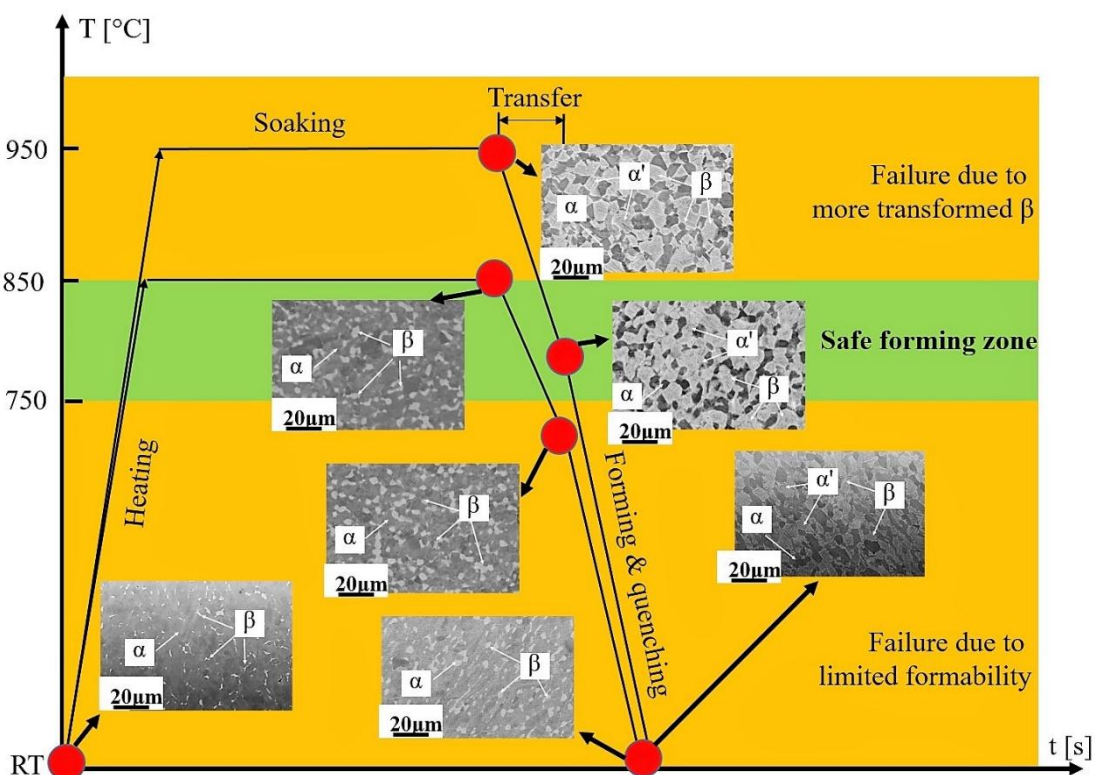


**Fig. 19** Evolution of microstructure during the forming process at 850°C and 950°C.

Control of the phase transformation during heating and improving the forming temperature are the two basic guidelines to further extend the processing window. The transformed  $\beta$  would impair the ductility of the material, therefore in order to reduce the phase transformation during heating, a reduction of soaking time should be considered. It will also prevent the precipitation of secondary  $\alpha$  phase within the structure, when the temperature will be great enough to initiate the phase transformation. On the other hand, the formability of the material could also be improved by using warm forming tools to reduce the temperature reduction during the forming process. It also should be mentioned that at elevated temperatures, oxidation became an obvious problem. This phenomenon

may also reduce the formability and increase the hardness of material during forming. In order to prevent oxidation during the forming, the use of high quality oxidation resistant lubricant coating should be considered.

## 5. Conclusions

In this study, the formability and microstructure evolution mechanisms during a novel hot stamping process for titanium alloys using cold forming tools and a hot blank were investigated. During uniaxial tensile tests, a satisfactory elongation of the material ranging from 30% to 60% was achieved at temperatures ranging from 750 to 900°C. The main microstructure evolution mechanisms during deformation were recovery, phase transformation and recrystallization. The hardness of the material after deformation first decreased with the temperature due to recovery, and subsequently increased due to the phase transformation. During the hot stamping tests, titanium parts were successfully formed at heating temperatures ranging from 750 to 850°C. Forming at temperatures lower than 750°C, failed due to limited ductility of the material. At heating temperatures above 900°C, significant phase transformation occurred. During the following transfer and forming, temperature reduction led to formation of transformed  $\beta$ , formability reduction and subsequent failure. The post-form hardness distribution demonstrated the same tendency as that after uniaxial tensile test. The post-form mechanical properties and microstructure were mainly determined by heating temperature and soaking time, hence formability and post-form properties of the material could be tailored through the adjustment of the forming process. In order to extend the processing window, measures such as reduction of soaking time, use of warm forming tools and oxidation resistant lubricants during the hot stamping process should be considered.

## Acknowledgements

The strong support from the Aviation Industry Corporation of China (AVIC) Beijing Aeronautical Manufacturing Technology Research Institute (BAMTRI) for this funded research is much appreciated. The research was performed at the AVIC Centre for Structural Design and Manufacture at Imperial College London.

## References

- [1] M. Peters, J. Kumpfert, C.H. Ward, C. Leyens, Titanium alloys for aerospace applications, *Adv. Eng. Mater.* 5 (2003) 419–427. doi:10.1002/adem.200310095.
- [2] D. Serra, Superplastic Forming Applications on Aero Engines . A review of ITP Manufacturing Processes, *EuroSPF08* (2009) hal-00359685, version 1.

## ACCEPTED MANUSCRIPT

- [3] H. Yang, X.G. Fan, Z.C. Sun, L.G. Guo, M. Zhan, Recent developments in plastic forming technology of titanium alloys, *Sci. China Technol. Sci.* 54 (2011) 490–501.  
doi:10.1007/s11431-010-4206-y.
- [4] A. Astarita, E. Armentani, E. Ceretti, L. Giorleo, P. Mastrilli, V. Paradiso, F. Scherillo, A. Squillace, C. Velotti, Hot Stretch Forming of a Titanium Alloy Component for Aeronautic: Mechanical and Modeling, *Key Eng. Mater.* 554–557 (2013) 647–656.  
doi:10.4028/www.scientific.net/KEM.554-557.647.
- [5] T. Deng, D. Li, X. Li, P. Ding, K. Zhao, Hot stretch bending and creep forming of titanium alloy profile, *Procedia Eng.* 81 (2014) 1792–1798. doi:10.1016/j.proeng.2014.10.234.
- [6] K. Wang, G. Liu, K. Huang, D.J. Politis, L. Wang, Effect of recrystallization on hot deformation mechanism of TA15 titanium alloy under uniaxial tension and biaxial gas bulging conditions, *Mater. Sci. Eng. A.* 708 (2017) 149–158. doi:10.1016/j.msea.2017.09.128.
- [7] T. Raghu, I. Balasundar, M. Sudhakara Rao, Isothermal and near isothermal processing of titanium alloys, *Def. Sci. J.* 61 (2011) 72–80. doi:10.14429/dsj.61.321.
- [8] A.G. Ermachenko, R.Y. Lutfullin, R.R. Mulyukov, Advanced technologies of processing titanium alloys and their applications in industry, *Rev. Adv. Mater. Sci.* 29 (2011) 68–82.
- [9] Z. Hamedon, K. Mori, T. Maeno, Hot Stamping of Titanium Alloy Sheet Using Resistance Heating, *NMSTU*, 5 (2013) 12–15.
- [10] J. Liu, H. Gao, O. El Fakir, L. Wang, J. Lin, HFQ forming of AA6082 tailor welded blanks, 4th Int. Conf. New Form. Technol. 5006 (2015) 6082. doi:10.1051/matecconf/20152105006.
- [11] P.F. Bariani, S. Bruschi, A. Ghiotti, F. Michieletto, Hot stamping of AA5083 aluminium alloy sheets, *CIRP Ann. - Manuf. Technol.* 62 (2013) 251–254. doi:10.1016/j.cirp.2013.03.050.
- [12] T. Maeno, K. ichiro Mori, R. Yachi, Hot stamping of high-strength aluminium alloy aircraft parts using quick heating, *CIRP Ann. - Manuf. Technol.* 66 (2017) 269–272.  
doi:10.1016/j.cirp.2017.04.117.
- [13] J.D. Beal, R. Boyer, D. Sanders, T.B. Company, Forming of Titanium and Titanium Alloys, *ASM Handb. Metalwork. Sheet Form.* 14B (2006) 656–669. doi:10.1361/asmhba0005146.
- [14] J.C. Williams, E.A. Starke, Progress in structural materials for aerospace systems, *Acta Mater.* 51 (2003) 5775–5799. doi:10.1016/j.actamat.2003.08.023.
- [15] J. Sieniawski, W. Ziaja, K. Kubiak, M. Motyka, Microstructure and Mechanical Properties of

## ACCEPTED MANUSCRIPT

High Strength Two-Phase Titanium Alloys, in J. Sieniawski (Ed.), Titanium Alloys - Advances in Properties Control, InTech, 2013. pp.69-80 DOI: 10.5772/56197.

- [16] G. Quan, G. Luo, J. Liang, D. Wu, A. Mao, Q. Liu, Modelling for the dynamic recrystallization evolution of Ti – 6Al – 4V alloy in two-phase temperature range and a wide strain rate range, *Comput. Mater. Sci.* 97 (2015) 136–147. doi:10.1016/j.commatsci.2014.10.009.
- [17] D.R. Tobergte, S. Curtis, Recrystallisation and Related Annealing Phenomena, *J. Chem. Inf. Model.* 53 (2013) 1689–1699. doi:10.1017/CBO9781107415324.004.
- [18] Y.Q. Ning, X. Luo, H.Q. Liang, H.Z. Guo, J.L. Zhang, K. Tan, Competition between dynamic recovery and recrystallization during hot deformation for TC18 titanium alloy, *Mater. Sci. Eng. A.* 635 (2015) 77–85. doi:10.1016/j.msea.2015.03.071.
- [19] Q. Bai, J. Lin, T.A. Dean, D.S. Balint, T. Gao, Z. Zhang, Modelling of dominant softening mechanisms for Ti-6Al-4V in steady state hot forming conditions, *Mater. Sci. Eng. A.* 559 (2013) 352–358. doi:10.1016/j.msea.2012.08.110.
- [20] L. He, A. Dehghan-manshadi, R.J. Dippenaar, The evolution of microstructure of Ti – 6Al – 4V alloy during concurrent hot deformation and phase transformation, *Mater. Sci. Eng. A.* 549 (2012) 163–167. doi:10.1016/j.msea.2012.04.025.
- [21] T. Maeno, Y. Yamashita, K.-I. Mori, Hot Stamping of Titanium Alloy Sheets into U Shape with Concave Bottom and Joggle Using Resistance Heating, *Key Eng. Mater.* 716 (2016) 915–922. doi:10.4028/www.scientific.net/KEM.716.915.
- [22] F. Ozturk, R.E. Ece, N. Polat, A. Koksal, Z. Evis, A. Polat, Mechanical and microstructural evaluations of hot formed titanium sheets by electrical resistance heating process, *Mater. Sci. Eng. A.* 578 (2013) 207–214. doi:10.1016/j.msea.2013.04.079.
- [23] E.L. Odenberger, J. Hertzman, P. Thilderkvist, M. Merklein, A. Kuppert, T. Stöhr, J. Lechler, M. Oldenburg, Thermo-mechanical sheet metal forming of aero engine components in Ti-6Al-4V - PART 1: Material characterisation, *Int. J. Mater. Form.* 6 (2013) 391–402. doi:10.1007/s12289-012-1093-8.
- [24] B. Babu, L.-E. Lindgren, Dislocation density based model for plastic deformation and globularization of Ti-6Al-4V, *Int. J. Plast.* 50 (2013) 94–108. doi:10.1016/j.ijplas.2013.04.003.
- [25] S. Jadhav, A. Powar, S. Patil, A. Supare, B. Farane, R. Singh, Effect of volume fraction of alpha and transformed beta on the high cycle fatigue properties of bimodal Ti6Al4V alloy, *IOP Conf. Ser. Mater. Sci. Eng.* 201 (2017). doi:10.1088/1757-899X/201/1/012035.

**ACCEPTED MANUSCRIPT**

- [26] T. Furuhara, B. Poorganji, H. Abe, T. Maki, Dynamic recovery and recrystallization in titanium alloys by hot deformation, *Jom.* 59 (2007) 64–67. doi:10.1007/s11837-007-0013-8.
- [27] L. Saraf, Kernel Average Misorientation Confidence Index Correlation from FIB Sliced Ni-Fe-Cr alloy Surface, *Microsc. Microanal.* 17 (2011) 424–425. doi:10.1017/S1431927611002996.
- [28] L. Jiao, Microstructure Evolution during High Temperature Deformation of Ti-6Al-4V Alloy, *Rare Met. Mater. Eng.* 39 (2010) 1323–1328. doi:10.1016/S1875-5372(10)60114-2.

Accepted manuscript